Degradation Product Partitioning in Source Zones Containing Chlorinated Ethene Dense Non-Aqueous-Phase Liquid

C. ANDREW RAMSBURG,*,† CHRISTINE E. THORNTON,†,§ AND JOHN A. CHRIST‡

Department of Civil and Environmental Engineering, Tufts University, 200 College Avenue, Room 113 Anderson Hall, Medford, Massachusetts 02155, and Department of Civil and Environmental Engineering, U.S. Air Force Academy, Colorado Springs, Colorado 80840, United States

Received July 26, 2010. Revised manuscript received October 12, 2010. Accepted October 19, 2010.

Abiotic and biotic reductive dechlorination with chlorinated ethene dense non-aqueous-phase liquid (DNAPL) source zones can lead to significant fluxes of complete and incomplete transformation products. Accurate assessment of in situ rates of transformation and the potential for product sequestration requires knowledge of the distribution of these products among the solid, aqueous, and organic liquid phases present within the source zone. Here we consider the fluid−fluid partitioning of two of the most common incomplete transformation products, *cis*-1,2-dichloroethene (*cis*-DCE) and vinyl chloride (VC). The distributions of *cis*-DCE and VC between the aqueous phase and tetrachloroethene (PCE) and trichloroethene (TCE) DNAPLs, respectively, were quantified at 22 °C for the environmentally relevant, dilute range. The results suggest that partition coefficients (concentration basis) for VC and *cis*-DCE are 70 ± 1 $L_{aq}/L_{TCE\ DNAPL}$ and 105 ± 1 $L_{aq}/L_{PCE\ DNAPL}$, respectively. VC partitioning data (in the dilute region) were reasonably approximated using the Raoult's law analogy for liquid−liquid equilibrium. In contrast, data for the partitioning of *cis*-DCE were well described only when well-parametrized models for the excess Gibbs free energy were employed. In addition, available vapor−liquid and liquid−liquid data were employed with our measurements to assess the temperature dependence of the *cis*-DCE and VC partition coefficients. Overall, the results suggest that there is a strong thermodynamic driving force for the reversible sequestration of *cis*-DC and VC within DNAPL source zones. Implications of this partitioning include retardation during transport and underestimation of the transformation rates observed through analysis of aqueous-phase samples.

Introduction

The potential of reductive dechlorination processes to transform chlorinated contaminants to benign (or less toxic) compounds has attracted considerable interest within the subsurface remediation community. Source zones containing dense non-aqueous-phase liquids (DNAPLs) are of particular interest (*1*−*3*). Engineering enhancements made within DNAPL source zones, such as the supply of reactive metal particles or the stimulation of indigenous microbial populations, may provide an effective remediation strategy (e.g., refs *4* and *5*). Abiotic and biotic reductive dechlorination of chlorinated ethenes can proceed via hydrogenolysis, α-elimination, β-elimination, hydrogenation, and coupling pathways (*6*−*8*). While appreciable quantities of coupling products were reported in some metal-limited systems (e.g., refs *9* and *10*), heterogeneous and catalyzed reactions involving metals generally result in relatively rapid, complete dechlorination to ethene and ethane via a combination of β-elimination, hydrogenation, and hydrogenolysis reactions (*6*). Metabolic reductive dechlorination, however, proceeds via a slower, sequential hydrogenolysis pathway that can result in the accumulation of potentially more toxic chlorinated degradation products (*8*).

Transformation of a chlorinated ethene to ethene via metabolic reductive dechlorination requires a consortium of organisms, with complete transformation to ethene linked to the presence and activity of *Dehalococcoides* spp. (*5, 7*). Differences in electron donor availability and utilization, chlorinated ethene toxicity limits, and pH sensitivity among the multiple species required for the transformation of tetrachloroethene (PCE) and trichloroethene (TCE) to ethene are just some of the challenges to the effective engineering and management of this dechlorination strategy (*3, 5*). When the overall dechlorination process stalls (or fails to completely dechlorinate PCE and TCE), *cis*-dichloroethene (c*is*-DCE) and vinyl chloride (VC) accumulate at levels well above regulated concentrations (*3, 11*). Given that the production of *cis*-DCE and VC corresponds to the same molar extent as the amount of degradation of PCE (or TCE) and the presence of DNAPLs (even at low saturation) represents considerable mass, degradation products can approach millimolar concentrations (*11*).

While accumulation of *cis*-DCE and VC during DNAPL source zone treatment is strongly influenced by microbial transformation rates, it is important to recognize that the production of *cis*-DCE and VC is occurring within multiliquid environments. Thus, remediation design requires improved knowledge of the interplay between microbial transformation and degradation product partitioning (*12, 13*). In fact, degradation product partitioning may help explain mass balance and reactive transport anomalies reported in laboratory-scale, metabolic reductive dechlorination studies (e.g., refs *13*−*19*). Thus, the overall objective of this work is to elucidate the equilibrium distribution of VC and *cis*-DCE between the aqueous phase and chloroethene DNAPLs across a range of temperatures relevant to source zone remediation. The results reported here are used to illustrate the implications of degradation product partitioning within DNAPL source zones.

Materials and Methods

Chemicals. Vinyl chloride (gas, 99.5+% purity), *cis*-1,2-dichloroethene (97% purity), and tetrachloroethene (99% purity) were purchased from Sigma-Aldrich and used as received. Trichloroethene (99+% purity) was purchased from Acros Organics and used as received. Dimethyl sulfoxide (DMSO) (99.9% purity) was purchased from Fisher Scientific. DMSO was used to minimize volatilization and to ensure miscibility during sample preparation and analysis. Water

* Corresponding author phone: (617) 627-4286; fax: (617) 627-3994; e-mail: andrew.ramsburg@tufts.edu.
† Tufts University.
‡ U.S. Air Force Academy.
§ Now with the U.S. Peace Corps in Marcovia, Choluteca, Honduras.

Report Documentation Page

Form Approved
OMB No. 0704-0188

1. REPORT DATE	2. REPORT TYPE	3. DATES COVERED
12 OCT 2010		**00-00-2010 to 00-00-2010**

4. TITLE AND SUBTITLE	5a. CONTRACT NUMBER
Degradation Product Partitioning in Source Zones Containing Chlorinated Ethene Dense Non-Aqueous-Phase Liquid	5b. GRANT NUMBER
	5c. PROGRAM ELEMENT NUMBER
6. AUTHOR(S)	5d. PROJECT NUMBER
	5e. TASK NUMBER
	5f. WORK UNIT NUMBER
7. PERFORMING ORGANIZATION NAME(S) AND ADDRESS(ES) **U.S. Air Force Academy,Department of Civil and Environmental Engineering,Colorado Springs,CO,80840**	8. PERFORMING ORGANIZATION REPORT NUMBER
9. SPONSORING/MONITORING AGENCY NAME(S) AND ADDRESS(ES)	10. SPONSOR/MONITOR'S ACRONYM(S)
	11. SPONSOR/MONITOR'S REPORT NUMBER(S)

12. DISTRIBUTION/AVAILABILITY STATEMENT
Approved for public release; distribution unlimited

13. SUPPLEMENTARY NOTES

14. ABSTRACT

15. SUBJECT TERMS

16. SECURITY CLASSIFICATION OF:			17. LIMITATION OF ABSTRACT	18. NUMBER OF PAGES	19a. NAME OF RESPONSIBLE PERSON
a. REPORT	b. ABSTRACT	c. THIS PAGE			
unclassified	**unclassified**	**unclassified**	**Same as Report (SAR)**	**7**	

was purified using a Millipore Milli-Q Gradient A10 system to a resistivity of ≥18.2 MΩ·cm and total organic carbon of <15 ppb.

Batch Methods. Batch reactors containing Milli-Q water, TCE, and VC and those containing Milli-Q water, PCE, and *cis*-DCE were prepared in triplicate using Kimble 30 mL glass centrifuge tubes sealed with poly(tetrafluoroethene) (PTFE)/silicone septa and open-top screw caps. Because it was not practical to directly add the necessary mass of VC to the reactors in gaseous form, a sparging procedure was developed to create solutions of VC in TCE (Figure SI-1, Supporting Information). Given the carcinogenicity of VC, a management strategy was developed and implemented to ensure the safety of all personnel (see the Safety and VC Management section in the Supporting Information). Prior to using the VC-sparged TCE, the VC concentration was quantified in the TCE solution using the analytical methods described below.

Reactors, containing approximately 20 mL of Milli-Q water and 10 mL of non-aqueous-phase liquid (NAPL) comprising various amounts of TCE and VC or PCE and *cis*-DCE, were equilibrated for a minimum of 72 h on LabQuake oscillating shaker trays at 22 ± 2 °C (VC studies) or 22 ± 0.1 °C (*cis*-DCE studies). Previous studies have determined this duration sufficient to reach equilibrium (*16, 20*). The difference in the level of temperature control employed in these studies resulted from safety precautions taken to ensure VC was contained within a ventilating fume hood. Reactors containing *cis*-DCE were allowed to mix within a constant-temperature room containing a recirculating fume hood. Following the period of equilibration, the tubes were centrifuged at 1500 rpm for 10 min to ensure separation of the aqueous phase and organic phases (*20*). Aqueous-phase and NAPL samples were collected in triplicate for subsequent analysis. Subsequent to sampling each reactor for composition, additional samples of both phases were collected for quantification of density. Densities of the aqueous and organic phases were determined in triplicate using 2 mL glass pycnometers calibrated daily using Milli-Q water at 22 ± 2 °C.

Solubility Measurements. The aqueous solubility of *cis*-DCE was determined as described above with reactors containing only water and excess, neat *cis*-DCE. The aqueous solubility of VC could not be determined in this manner. Thus, VC gas was sparged through Milli-Q water at 22 ± 2 °C for no less than 30 min using the previously described apparatus (Figure SI-1, Supporting Information). Samples of the aqueous phase were then collected in quadruplicate. The sampling was repeated twice more after two 10 min periods of sparging to produce quadruplicate samples at three sparging durations (or 12 total samples).

Analytical Methods. Triplicate samples of the aqueous phase (20−70 uL) and NAPL (20−50 uL) were collected from the reactors containing VC using a gastight syringe and transferred to sealed headspace vials for subsequent analysis as described below. NAPL samples were diluted into 1.8 mL of DMSO and then subsampled (10−50 uL) in triplicate to headspace vials for quantification. Dilutions were varied to be consistent with the linear response range of the analytical method. All VC samples and standards contained ∼10 mL of 22% (w/w) DMSO in Milli-Q water. For reactors containing *cis*-DCE, triplicate samples were collected from the aqueous phase (∼5 mL) and NAPL (∼20 μL). Aqueous-phase samples were diluted with 22 wt % DMSO in water to a total mass of 10 g. NAPL samples were diluted into 8 mL of DMSO, which was then subsampled and diluted with water (10× dilution to a total volume of 10 mL) to produce a sample for analysis that contained ∼11 wt % DMSO.

VC and *cis*-DCE concentrations were measured using a Hewlett-Packard 5890 series II gas chromatograph equipped with an HP Plot Q column (30 m × 0.530 mm), a flame ionization detector, and a Perkin-Elmer Turbo Matrix 40 Trap headspace sampler. Headspace vials were heated to 95 °C, shaken for 24 min, and pressurized to 25 psi (via N_2 addition) by the headspace sampler prior to transfer of 3 mL of gas to the gas chromatograph for analysis. The instrument was calibrated prior to each day of use with a six-point calibration curve.

Thermodynamic Modeling. Partitioning of contaminants between aqueous and nonaqueous phases in the environment is frequently assumed to follow an analogy to Raoult's law, where the aqueous solubility of the contaminant is multiplied by the mole fraction of the contaminant in the nonaqueous phase to produce an effective solubility (*21*):

$$x_i^{\mathrm{aq}} = x_i^{\mathrm{aq,soly}} x_i^{\mathrm{NAPL}} \tag{1}$$

where x_i^{aq} and x_i^{NAPL} are the mole fractions of component i in the aqueous phase and NAPL, respectively, and $x_i^{\mathrm{aq,soly}}$ is the mole fraction representing the aqueous solubility of component i. Liquid−liquid equilibrium, however, is rigorously described by equating the fugacities of each liquid phase (*22*):

$$x_i^{\mathrm{aq}}\gamma_i^{\mathrm{aq}}\phi_i^0 P_i^0 \exp\left(\frac{\bar{v}_i^{\mathrm{L}}(P - P^0)}{RT}\right) = x_i^{\mathrm{NAPL}}\gamma_i^{\mathrm{NAPL}}\phi_i^0 P_i^0 \times \exp\left(\frac{\bar{v}_i^{\mathrm{L}}(P - P^0)}{RT}\right) \tag{2}$$

where γ_i^{aq} and γ_i^{NAPL} are the activity coefficients of component i in the aqueous phase and NAPL, respectively, ϕ_i^0 is the fugacity coefficient of component i at the vapor pressure P_i^0 (the reference state for component i), $\bar{v}_i^{\mathrm{L}}$ is the liquid-phase, partial molar volume of component i, R is the universal gas constant, and T is the temperature (K). It should be recognized that the activity coefficient in each phase is a function of x_i and that the Poynting correction (i.e., the exponential function) corrects for the weak pressure dependence of the activity coefficient.

If the aqueous-phase mole fraction of component i falls within the dilute solution approximation, then γ_i^{aq} can be replaced by the infinite dilution activity coefficient, $\gamma_i^{\infty,\mathrm{aq}}$. A similar substitution ($\gamma_i^{\infty,\mathrm{NAPL}}$) can be made for γ_i^{NAPL} if the values of x_i^{NAPL} permit a dilute solution approximation. Under these conditions, the liquid-phase molar volume of the pure component, v_i^{L}, may be used to approximate $\bar{v}_i^{\mathrm{L}}$ (*22*). Thus, these conditions produce a ratio of mole fractions that is constant and equal to the partition coefficient (on a mole fraction basis) for the dilute region, $K_{\mathrm{p}}^{x_i,\mathrm{dil}}$ (eq 3):

$$\frac{x_i^{\mathrm{NAPL}}}{x_i^{\mathrm{aq}}} = \frac{\gamma_i^{\infty,\mathrm{aq}}}{\gamma_i^{\infty,\mathrm{NAPL}}} = K_{\mathrm{p}}^{x_i,\mathrm{dil}} \tag{3}$$

In systems where the dilute solution approximation holds for the aqueous phase but is inappropriate (or questionable) for the NAPL, Henry's law may be employed to describe the aqueous-phase composition in equilibrium with a hypothetical real gas (*22*):

$$\phi_i p_i = H_i|_{P_{\mathrm{ref}}} x_i \exp\left(\frac{v_i^{\mathrm{L}}(P - P_{\mathrm{ref}})}{RT}\right) \tag{4}$$

In eq 4, ϕ_i is the gas-phase fugacity coefficient of component i, p_i is the partial pressure of component i in the gas phase, and P_{ref} is the reference pressure at which the Henry law coefficient, H_i, is defined (often taken to be P_i^0). The weak pressure dependence of H_i is accounted for using the Poynting correction, again assuming that v_i^{L} is an adequate approximation for $\bar{v}_i^{\mathrm{L}}$ at infinite dilution. For

systems of m components the Henry law coefficient for component i in the mixture, $H_{i,\mathrm{mix}}$, is defined as (*22*)

$$\ln H_{i,\mathrm{mix}} = \sum_{\substack{j=1\\ j\neq i}}^{m} x_j \ln H_{2,j} - \sum_{\substack{j=1\\ j\neq i}}^{m-1} \sum_{\substack{k>j\\ k\neq i}}^{m} a_{jk} x_j x_k \tag{5}$$

where a_{jk} are interaction parameters between the jth and kth components. Many multicomponent systems of environmental relevance contain dilute solutes, so $H_{i,\mathrm{mix}}$ can be well approximated as the Henry's coefficient for the binary, H_{ij} (e.g., water and volatile contaminant), where the solute and solvent are components i and j, respectively.

The fugacity coefficient in the gas phase can be calculated using the second virial coefficient and a Pitzer expansion as (*22*)

$$\ln \phi_i = \frac{P}{RT}\left(2\sum_{j=1}^{m} y_j \frac{RT_{\mathrm{c},ij}}{P_{\mathrm{c},ij}}(B^0_{ij} + \omega_{ij}B^1_{ij}) - \sum_{i=1}^{m}\sum_{j=1}^{m} y_i y_j \frac{RT_{\mathrm{c},ij}}{P_{\mathrm{c},ij}}(B^0_{ij} + \omega_{ij}B^1_{ij})\right) \tag{6a}$$

with

$$B^0_{ij} = \left(0.083 - 0.422\left(\frac{T_{\mathrm{c},ij}}{T}\right)^{1.6}\right) \tag{6b}$$

$$B^1_{ij} = \left(0.139 - 0.172\left(\frac{T_{\mathrm{c},ij}}{T}\right)^{4.2}\right) \tag{6c}$$

where y_i and y_j are the mole fractions of components i and j in the gas phase, T is the temperature, and $T_{\mathrm{c},ij}$ and $P_{\mathrm{c},ij}$ are the critical temperature and pressure, respectively, of the mixture formed by components i and j. $T_{\mathrm{c},ij}$ and $P_{\mathrm{c},ij}$ are defined using standard mixing rules (*22*).

Use of Henry's law (eq 4) to describe the aqueous-phase fugacity in eq 2 produces the following equation, which describes the partitioning of a solute that is assumed to be dilute within the aqueous phase:

$$\frac{x_i^{\mathrm{NAPL}}}{x_i^{\mathrm{aq}}} = \frac{H_i|_P}{\gamma_i^{\mathrm{NAPL}}\phi_i^0 P_i^0 \exp\left(\dfrac{\bar{v}_i^L(P - P^0)}{RT}\right)} = K_{\mathrm{p}}^{x_i} \tag{7}$$

While $K_{\mathrm{p}}^{x_i}$ is often a function of the composition (*20*), it can become constant when γ_i^{NAPL} is not a function (or is a weak function) of the NAPL composition, usually under an ideal solution assumption ($\gamma_i^{\mathrm{NAPL}} = 1$). If the NAPL is assumed to be an ideal solution (i.e., $\gamma_i^{\mathrm{NAPL}} = 1$), eq 7 can be simplified to produce the Raoult law analogy (RLA) (eq 8) for partitioning of component i between a dilute aqueous phase and an ideal NAPL.

$$\frac{x_i^{\mathrm{NAPL}}}{x_i^{\mathrm{aq}}} = \frac{H_i|_P}{\phi_i^0 P_i^0 \exp\left(\dfrac{\bar{v}_i^L(P - P^0)}{RT}\right)} = K_{\mathrm{p}}^{x_i,\mathrm{RLA}} \tag{8}$$

Comparison of eqs 1 and 8 defines $K_{\mathrm{p}}^{x_i,\mathrm{RLA}}$ as the inverse of $x_i^{\mathrm{aq,soly}}$. It should be noted, however, that the reference state for component i is treated as a real gas; thus, Raoult's law is never strictly applied. The RLA simply represents an analogy between eq 1 and that of Raoult's law. Alternatively, the partition coefficient can be (i) quantified by regressing liquid−liquid equilibrium data at a specific temperature or (ii) estimated for any set of conditions (including the limiting conditions that produce $K_{\mathrm{p}}^{x_i,\mathrm{dil}}$ and $K_{\mathrm{p}}^{x_i,\mathrm{RLA}}$) using a group contribution method (e.g., UNIFAC) to simulate liquid activity coefficients for use in an isothermal flash calculation.

Use of the RLA to calculate the partition coefficient implies that the Henry law coefficient is known at all temperatures of interest. The temperature dependence of Henry's law coefficients is frequently modeled using the Van't Hoff equation, which performs well over a small temperature range where the partial molar enthalpy of volatilization can be assumed to be constant. This assumption, however, fails for most solutes over an expanded range of temperatures, resulting in the use of empirical descriptions for the temperature dependence of Henry's law coefficients (*22, 23*). Recently, an empirical model (eq 9) was employed to describe the Henry law coefficients for organic solutes in water by assuming that the partial molar enthalpy of volatilization is a linear function of the temperature (*23*).

$$H_i = \exp\left(A - \frac{B}{T} + C\ln T\right) \tag{9}$$

A, B, and C in eq 9 are fitting parameters. Regression of eq 9 to existing H_i data was accomplished using a weighted least-squares approach (*24*). A 10% relative standard error was assumed for all data sets not reporting uncertainty.

Results and Discussion

Use of the RLA requires reliable values of the aqueous solubility. Thus, existing data were reviewed and reanalyzed to develop new correlations for the temperature dependence of the Henry law coefficient (and hence solubility) describing the partitioning of VC and *cis*-DCE between aqueous and gas phases. Data are available in the form of vapor−liquid equilibria or liquid−liquid equilibria (*13, 25−34*), EPICS data (*35, 36*), and infinite dilution activity coefficients (*37, 38*). Many of these vapor−liquid equilibria and EPICS studies, however, overlook nonidealities in the gas phase that are known to exist for VC and to a lesser extent *cis*-DCE (*25*) and were therefore reanalyzed using eq 4. The EPICS equation for a nonideal gas phase (eq SI-4, Supporting Information) was developed using the concentration form of eq 4 and system mass balance following the derivation provided by Gossett (*35*).

Regressions were accomplished using H_i and are shown in Figures SI-2 and SI-3 (Supporting Information) in terms of the concentration form of the Henry law coefficient, H_i^C, which assumes that the molar density of the solution can be approximated by the molar density of the solvent (i.e, the solute is dilute enough to have a negligible influence on the physical properties of the solution). This assumption was valid for VC and *cis*-DCE as the measured densities were within 0.2% of the corresponding density of water. Values for the parameters in eq 9 were found to be $A = 214.8$, $B = 11\,688$, and $C = -29.6$ for VC ($R^2 = 0.98$) and $A = 182.0$, $B = 11\,158$, and $C = -24.4$ for *cis*-DCE ($R^2 = 0.86$). The lower R^2 value in the case of *cis*-DCE results from the large variability in the measured values of H_i over a limited range of temperature (Figure SI-3). The correlations developed here offer the improvements of greater data support and greater temperature range when compared to previously reported correlations (*35, 36*). Use of the correlations is appropriate for temperatures of 0.2−85 °C for VC and 10−40 °C for *cis*-DCE—an important advance when assessing partitioning (gas−liquid, solid−liquid, or liquid−liquid) where contaminant reduction follows thermal remediation (e.g., refs *39* and *40*).

Aqueous solubilities of VC and *cis*-DCE (in mole fraction) calculated using eq 2 and the correlations developed for the Henry law coefficients (at 1 atm) are shown as a function of temperature in Figures 1 and 2. Mole fractions were converted to concentration by assuming that the presence of VC or

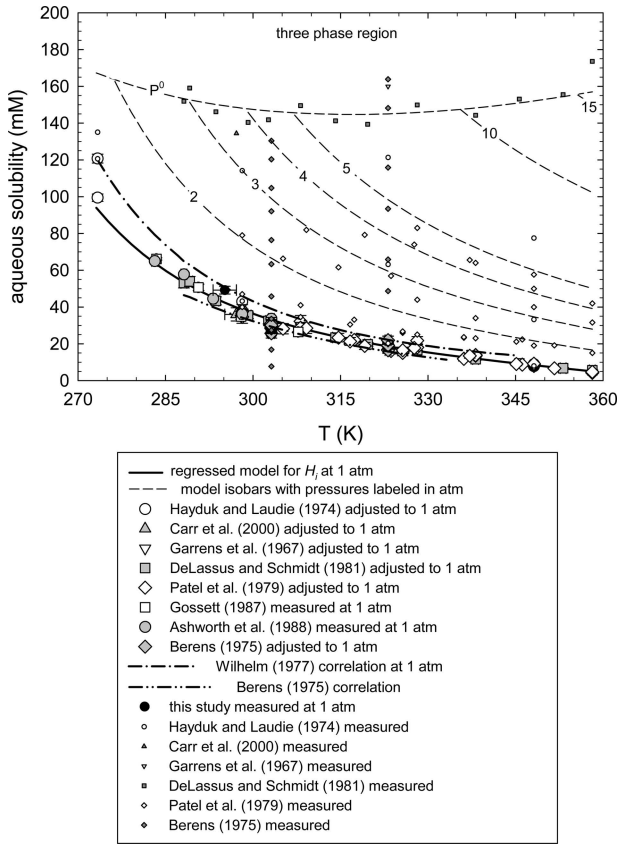

FIGURE 1. Solubility of vinyl chloride in water. Error bars (standard error) are included for data at 1 atm only. Many error bars are smaller than the associated symbol.

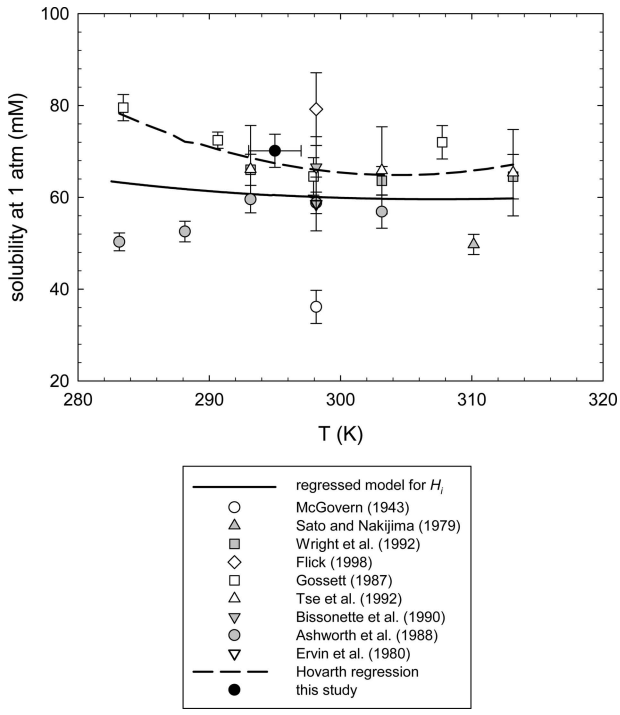

FIGURE 2. Solubility of *cis*-DCE in water. Error bars represent the standard error.

cis-DCE had a negligible influence on the molar volume of the aqueous solution. The solubility of VC was available at total pressures ranging from 0.32 to 17.4 atm (Figure 1). Each value for solubility was adjusted using the Henry law coefficient at 1 atm and a total pressure of 1 atm for a binary

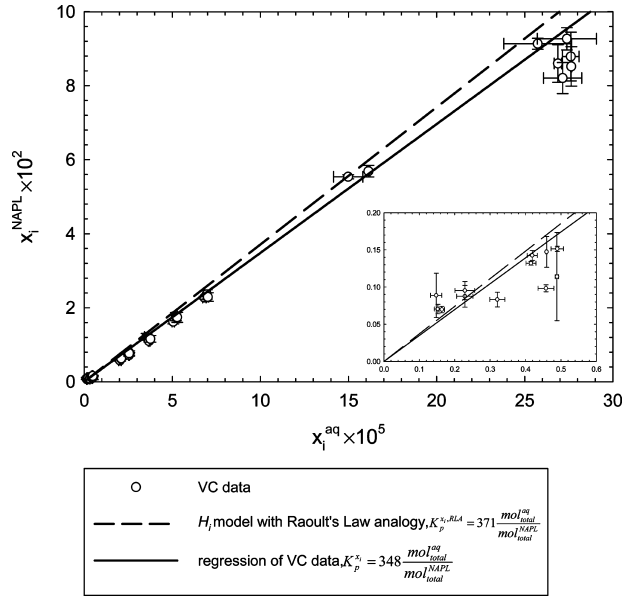

FIGURE 3. Equilibrium distribution of vinyl chloride between an aqueous phase and TCE NAPL at 22 ± 2 °C. The inset provides better visualization of x_i^{aq} data below 6 × 10^{-6}. Error bars represent the standard error established from triplicate sampling of the same reactor.

system of VC and water (eq 2). In the case of VC, the pressure dependence of the gas solubility is shown as a series of isobars in Figure 1 and contours in Figure SI-4 (Supporting Information). Also shown in Figure 1 are two correlations for the aqueous solubility that were developed in the 1970s by regressing subsets of these solubility data. The new correlation (in the form of a Henry law coefficient) better captures the large data set and offers a larger range of applicable temperatures. Comparison of the measured aqueous solubility of VC (49 ± 2 mM at 22 ± 2 °C and 1 atm) to that predicted from the new correlation at 1 atm and 22 °C (42.4 mM) suggests the measurement may be high. Note that values of H_i calculated using these measured solubilities are shown in Figures SI-2 and SI-3 (Supporting Information), but the measurements were not employed in the regression. It is likely that the discrepancy between the measured VC solubility and literature values resulted from a pressure in the sparging apparatus that was slightly greater than 1 atm (headspace pressures were not monitored). Also, it is important to recognize that the assumption of 1 atm of total pressure also means that there is no NAPL present (note the solubility curve at the vapor pressure P^0 in Figure 1). Any system containing NAPL requires use of the aqueous solubility corresponding to the vapor pressure of VC (see Table SI-1, Supporting Information, for Antoine equation parameters). The measured value for the aqueous solubility of *cis*-DCE (70 ± 4 mM at 22 ± 2 °C) appears to fall within the scatter in the literature values, but is noted to be higher than that predicted by the correlation at 22 °C (60.5 mM).

A series of batch, liquid−liquid equilibrium experiments were employed to measure the distribution of VC in TCE NAPL and *cis*-DCE in PCE DNAPL. Data from these experiments are shown in Figures 3 and 4, respectively, in terms of mole fractions. The insets in each figure show the lower concentration region of each plot. Regressions (linear least-squares weighted by the relative standard error) were used to determine $K_p^{x_i}$ for VC (348 ± 4, $R^2 = 0.99$) and *cis*-DCE (593 ± 5, $R^2 = 0.99$). These regressions assume that the partition coefficient was not a strong function of the composition. The regressed values for the partition coefficients for VC between an aqueous phase and TCE DNAPL and for *cis*-DCE between an aqueous phase and PCE DNAPL can be ap-

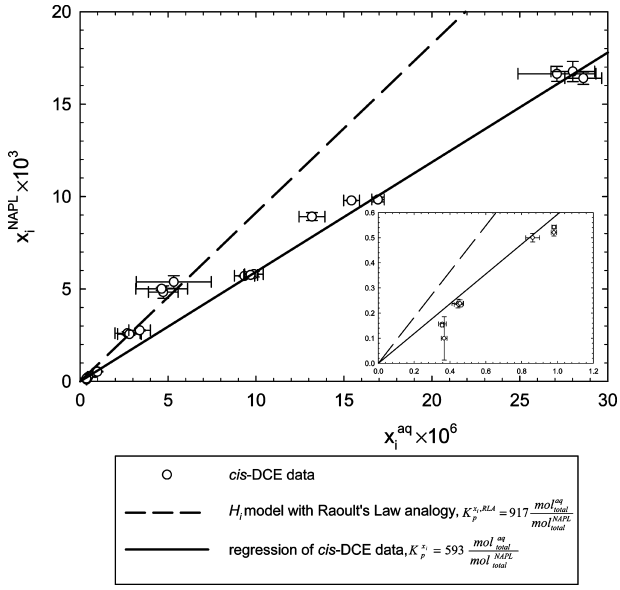

FIGURE 4. Equilibrium distribution of *cis*-1,2-dichloroethene between an aqueous phase and PCE DNAPL at 22 ± 0.1 °C. The inset provides better visualization of x_i^{aq} data below 1.2 × 10^{-6}. Error bars represent the standard error established from triplicate sampling of the same reactor.

proximated on a concentration basis ($K_p^{C_i}$) by 70 ± 1 $L_{aq}/L_{TCE\ DNAPL}$ and 105 ± 1 $L_{aq}/L_{PCE\ DNAPL}$, respectively.

Alternatively, UNIFAC (*41, 42*) estimates of the ratio of infinite dilution activity coefficients ($K_p^{x_i,dil}$) are 60 and 644 for VC and *cis*-DCE, respectively (not plotted). It is hypothesized that the poor performance of UNIFAC when estimating the partitioning of VC relates to the use of compounds with lower vapor pressures ($\ll P^0_{VC} = 3.65$ atm at 22 °C) when regressing the interaction parameters between groups 7 (water) and 37 (C═CCl) (e.g., refs *42* and *43*). This hypothesis is supported by the considerably better UNIFAC estimate of the partition coefficient for *cis*-DCE, which is within 10% of the measured value. In addition, this hypothesis suggests that UNIFAC may be employed to estimate *cis*-DCE partitioning in TCE NAPL.

Application of the RLA produces values for $K_p^{x_i,RLA}$ of 371 and 917 for VC and *cis*-DCE, respectively (Figures 3 and 4). The RLA estimate of the VC partition coefficient appears to describe the data well, especially if data that fall within 25 × 10^{-5} > x_i^{aq} > 30 × 10^{-5} influenced the regression to produce a lower value of $K_p^{x_i}$, although exclusion of these data from the regression produced a statistically insignificant change to the partition coefficient ($p = 0.34$). While the RLA is not capable of exactly reproducing the data, it does provide a reasonable first approximation (±10%) for the partitioning of VC between the aqueous phase and NAPL. Use of the RLA (eq 8) may prove advantageous given that estimates (on a mole fraction basis) are independent of the NAPL composition (recall that the RLA presumes the NAPL is an ideal solution). Estimates of $K_p^{x_i,RLA}$ for VC over the range of temperatures (0.2−85 °C) supporting the H_i model are consolidated using the following equation:

$$K_{p,VC}^{x_i} = -2.04 \times 10^3 + 15.3T - (2.43 \times 10^{-2})T^2 \quad 273.35\ K > T > 358.15\ K \quad (10)$$

The poor performance of the RLA for *cis*-DCE may be attributable to the scatter in the data used to parametrize the H_i model (Figure SI-3, Supporting Information). Use of the Gossett correlation (which produces lower values) to estimate H_i for *cis*-DCE improves the RLA estimate (759), but does not capture the data. UNIFAC performs better for *cis*-DCE than for VC, providing a reasonable first approximation

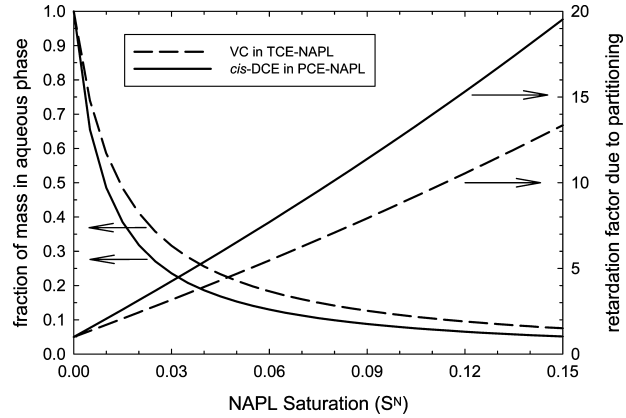

FIGURE 5. Reversible sequestration of products as a function of NAPL saturation: fraction of mass represented by the aqueous-phase concentration and retardation factor due to partitioning.

for the partition coefficient. UNIFAC was employed with established temperature dependencies of the mutual solubilities of PCE and water (*44*) to estimate the temperature dependence of the partition coefficient for *cis*-DCE in PCE DNAPL source zones (eq 11).

$$K_{p,cis\text{-}DCE}^{x_i} = 6.659 \times 10^3 - 33.76T + (4.536 \times 10^{-2})T^2 \quad 273.15\ K > T > 343.15\ K \quad (11)$$

These new correlations (eqs 10 and 11) along with the supporting data and analysis provide additional information necessary to better understand the distribution of contaminants and their degradation products in multiphase subsurface environments typical of those found at chlorinated DNAPL source zones for a variety of environmentally relevant temperatures.

Implications. Partitioning of degradation products within DNAPL source zones has the potential to reversibly sequester product mass. Reversible sequestration may have two important implications: (i) product mass located within the NAPL will likely be neglected when assessing degradation kinetics and (ii) the transport of degradation product downgradient may be retarded (due to partitioning). These implications are illustrated using the measured partition coefficients for VC and *cis*-DCE to calculate the fraction of total mass that is located within the aqueous phase (eq SI-9, Supporting Information) and the retardation factor (eq SI-10, Supporting Information) for a range of NAPL saturations assuming local equilibrium (Figure 5). If partitioning is fast relative to degradation, as accumulation of *cis*-DCE and VC may suggest, then laboratory and field assessments of degradation kinetics in the presence of NAPL may exclude large fractions of mass (e.g., aqueous-phase concentrations account for <40% of the total product mass at the modest NAPL saturation of 2%).

Several authors have suggested degradation product partitioning as a competing process that influences parent and product availability and, hence, apparent rates of degradation (*13, 15−17, 45, 46*). Thus, the influence of degradation product partitioning on the metabolic reductive dechlorination process occurring within a PCE DNAPL source zone was assessed using illustrative simulations. Here, the model and kinetic parameters described by Christ and Abriola (*46*) are employed to simulate a 30 cm column in which the first 15 cm contains entrapped PCE DNAPL at a uniform saturation of 2% (simulations are summarized in the Supporting Information). Partitioning was observed to produce pseudosteady effluent concentrations of *cis*-DCE and PCE that are approximately 40% and 90%, respectively, of the effluent concentrations produced in

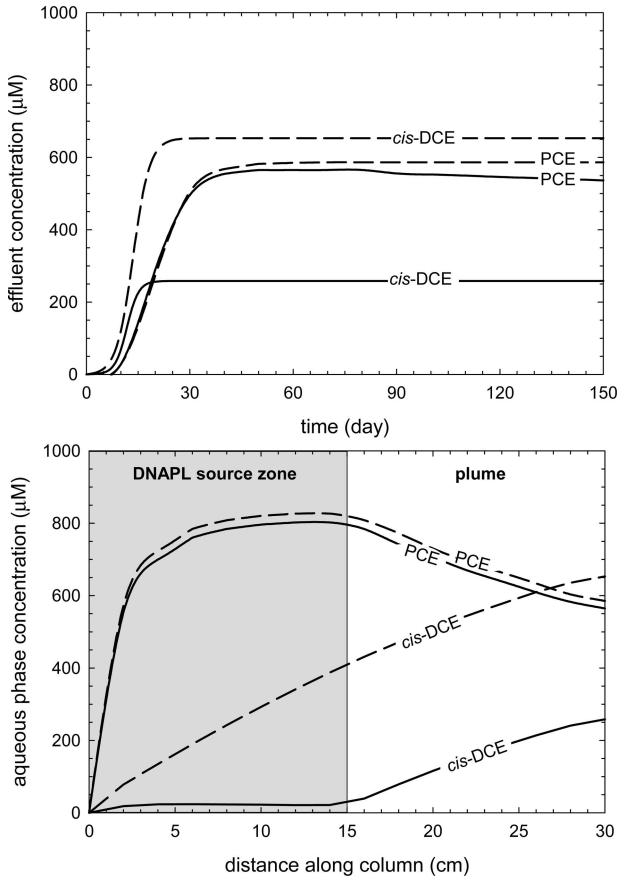

FIGURE 6. Effluent concentrations (top) and pseudo-steady-state resident aqueous-phase concentrations at 150 days (bottom) for simulations conducted with (solid line) and without (dashed line) degradation product partitioning. The column is 30 cm long with a PCE DNAPL source zone ($s^N = 0.02$) located in the first 15 cm. TCE concentrations (not shown) are below 5 μM.

the absence of partitioning (Figure 6). In addition, resident aqueous-phase concentrations (shown at 150 days) demonstrate partitioning attenuates *cis*-DCE concentrations within the 15 cm PCE DNAPL source zone (Figure 6). While the interplay between partitioning and degradation requires further study, the results suggest that transformation rates may be underestimated and remediation systems may be underdesigned when degradation product partitioning is neglected.

Recognition that reversible sequestration may influence assessments of degradation kinetics requires reassessment of dosing requirements (both the total amount and the rate of addition) when employing soluble substrate to produce the required electron donor. The introduction of insoluble substrate such as vegetable oils within the source zone (or immediately downgradient) may only accentuate the reversible sequestration (*12, 15, 19*). Absorption of degradation products (and parent contaminants) by insoluble amendments, while temporally decreasing the mass discharge, may, in fact, make difficult the assessment of the actual kinetics and extents (contaminant mass transformed) of the degradation process. Ongoing efforts are aimed at elucidating partitioning kinetics in NAPL source zones so that the interplay between partitioning and degradation can be rigorously assessed.

Acknowledgments

Support was provided by the National Science Foundation under Grants EAR 0711344 and EAR 0711450. Any opinions, findings, and conclusions or recommendations expressed in this material are those of the authors and do not necessarily reflect the views of the National Science Foundation. Additional support was received in the form of a Cataldo Fellowship awarded to C.E.T. by the Department of Civil and Environmental Engineering at Tufts University. We gratefully acknowledge the constructive comments provided by the reviewers.

Supporting Information Available

Safety and VC management plan, sparging apparatus diagram, regression of Henry's coefficients, VC solubility contour plot, Antoine parameters, temperature dependence of densities, aqueous fraction and retardation equations, and simulation description. This material is available free of charge via the Internet at http://pubs.acs.org.

Literature Cited

(1) Stroo, H. F.; Unger, M.; Ward, C. H.; Kavanaugh, M. C.; Vogel, T. M.; Leeson, A.; Marqusee, J. A.; Smith, B. P. Remediation chlorinated solvent source zones. *Environ. Sci. Technol.* **2003**, *37*, 224A–230A.

(2) Christ, J. A.; Ramsburg, C. A.; Löffler, F. E.; Pennell, K. D.; Abriola, L. M. Coupling aggressive mass removal with microbial reductive dechlorination for remediation of DNAPL source zones—A review and assessment. *Environ. Health Perspect.* **2005**, *113*, 465–477.

(3) Interstate Technology & Regulatory Council (ITRC). *In Situ Bioremediation of Chlorinated Ethene: DNAPL Source Zones*; ITRC: Washington, DC, 2008.

(4) Karn, B.; Kuiken, T.; Otto, M. Nanotechnology and in situ remediation: A review of the benefits and potential risks. *Environ. Health Perspect.* **2009**, *117* (12), 1823–1831.

(5) Aulenta, F.; Majone, M.; Tanoi, V. Review: Enhanced anaerobic bioremediation of chlorinated solvents: Environmental factors influencing microbial activity and their relevance under field conditions. *J. Chem. Technol. Biotechnol.* **2006**, *81*, 1463–1474.

(6) Arnold, W. A.; Roberts, A. L. Pathways and kinetics of chlorinated ethylene and chlorinated acetylene reation with Fe(0) particles. *Environ. Sci. Technol.* **2000**, *34*, 1794–1805.

(7) Löffler, F. E.; Edwards, E. A. Harnessing microbial activities for environmental cleanup. *Curr. Opin. Biotechnol.* **2006**, *17*, 274–284.

(8) Smidt, H.; de Vos, W. M. Anaerobic microbial dehalogenation. *Annu. Rev. Microbiol.* **2004**, *58*, 43–73.

(9) Liu, Y. Q.; Majetich, S. A.; Tilton, R. D.; Sholl, D. S.; Lowry, G. V. TCE dechlorination rates, pathways, and efficiency of nanoscale iron particles with different properties. *Environ. Sci. Technol.* **2005**, *39*, 1338–1345.

(10) Berge, N. D.; Ramsburg, C. A. Iron-mediated trichloroethene reduction within nonaqueous phase liquid. *J. Contam. Hydrol.*, in press.

(11) Interstate Technology & Regulatory Council (ITRC). *In Situ Bioremediation of Chlorinated Ethene DNAPL Source Zones: Case Studies*; ITRC: Washington, DC, 2007.

(12) Pfeiffer, P.; Bielefeldt, A. R.; Illangasekare, T.; Henry, B. Partitioning of dissolved chlorinated ethenes into vegetable oil. *Water Res.* **2005**, *39*, 4521–4527.

(13) Carr, C. S.; Garg, S.; Hughes, J. B. Effect of dechlorinating bacteria on the longevity and composition of PCE-containing nonaqueous phase liquids under equilibrium dissolution conditions. *Environ. Sci. Technol.* **2000**, *34*, 1088–1094.

(14) Yang, Y.; McCarty, P. L. Biologically enhanced dissolution of tetrachloroethene DNAPL. *Environ. Sci. Technol.* **2000**, *34*, 2979–2984.

(15) Yang, Y.; McCarty, P. L. Comparison between donor substrates for biologically enhanced tetrachloroethene DNAPL dissolution. *Environ. Sci. Technol.* **2002**, *36* (15), 3400–3404.

(16) Cope, N.; Hughes, J. B. Biologically-enhanced removal of PCE from NAPL source zones. *Environ. Sci. Technol.* **2001**, *35*, 2014–2021.

(17) Amos, B. K.; Christ, J. A.; Abriola, L. M.; Pennell, K. D.; Löffler, F. E. Experimental evaluation and mathematical modeling of microbially enhanced tetrachloroethene (PCE) dissolution. *Environ. Sci. Technol.* **2007**, *41* (3), 963–970.

(18) Amos, B. K.; Suchomel, E. J.; Pennell, K. D.; Löffler, F. E. Microbial activity and distribution during contaminant dissolution from an NAPL source zone. *Water Res.* **2008**, *42*, 2963–2974.

(19) Yu, S.; Semprini, L. Enhanced reductive dechlorination of PCE DNAPL with TBOS as a slow release electron donor. *J. Hazard. Mater.* **2009**, *167*, 97–104.

(20) Ramsburg, C. A.; Pennell, K. D. Density-modified displacement for dense nonaqueous phase liquid source-zone remediation: Density conversion using a partitioning alcohol. *Environ. Sci. Technol.* **2002**, *36*, 2082–2087.
(21) Banerjee, S. Solubility of organic mixtures in water. *Environ. Sci. Technol.* **1984**, *18* (8), 587–591.
(22) Prausnitz, J. M., Lichtenthaler, R. N. de Azevedo., E. G. *Molecular Thermodynamics of Fluid-Phase Equilibria*, 3rd ed.; Prentice Hall: Upper Saddle River, NJ, 1999.
(23) Lau, K.; Rogers, T. N.; Zei, D. A. Modeling the temperature dependence of Henry's law constant of organic solutes in water. *Fluid Phase Equilib.* **2010**, *290*, 166–180.
(24) Ramachandran, B. R.; Allen, J. M.; Halpern, A. M. The importance of weighted regression analysis in the determination of Henry's law constants by static headspace gas chromatography. *Anal. Chem.* **1996**, *68*, 281–286.
(25) Hayduk, W.; Laudie, H. Vinyl chloride gas compressibility and solubility in water and aqueous potassium laurate solutions. *J. Chem. Eng. Data* **1974**, *19* (3), 253–257.
(26) Garrens, H.; Fink, W.; Kohnlein, E. The kinetics of emulsion polymerization of vinyl chloride. *J. Polym. Sci., C* **1967**, *16*, 2781–2793.
(27) DeLassus, P. T.; Schmidt, D. D. Solubilities of vinyl chloride and vinylidene chloride in water. *J. Chem. Eng. Data* **1981**, *26*, 274–276.
(28) Patel, C. B.; Grandin, R. E.; Gupta, R.; Phillips, E. M.; Reynolds, C. E.; Chan, R. K. S. Partition coefficients of vinyl chloride between PVC/liquid/vapor phases. *Polym. J.* **1979**, *11* (1), 43–51.
(29) Berens, A. R. The solubility of vinyl chloride in poly(vinyl chloride). *Angew. Makromol. Chem.* **1975**, *47*, 97–110.
(30) McGovern, E. W. Chlorohydrocarbon solvents. *Ind. Eng. Chem.* **1943**, 1230–1239.
(31) Sato, A.; Nakajima, T. Structure activity relationships of some chlorinated hydrocarbons. *Arch. Envrion. Health* **1979**, *34*, 69–75.
(32) Flick, E. W. *Industrial Solvents Handbook*, 5th ed.; Noyes Data Corp.: Westwood, NJ, 1998.
(33) Ervin, A. L.; Mangone, M. A.; Singley, J. E. Trace organics removal by air stripping. *Proc.—Annu. Conf., Am. Water Works Assoc.* **1980**, 507–530.
(34) Bissonette, E. M.; Westrick, J. J.; Morand, J. M. Determination of Henry's coefficient for volatile organic compounds in dilute aqueous systems. *Proc.—Annu. Conf., Am. Water Works Assoc.* **1990**, 1913–1922.
(35) Gossett, J. M. Measurement of Henry's law constants for C1 and C2 chlorinated hydrocarbons. *Environ. Sci. Technol.* **1987**, *21*, 202–208.
(36) Ashworth, R. A.; Howe, G. B.; Mullins, M. E.; Rogers, T. N. Air-water partitioning coefficients of organics in dilute aqueous solutions. *J. Hazard. Mater.* **1988**, *18*, 25–36.
(37) Wright, D. A.; Sandler, S. I.; DeVoll, D. Infinite dilution activity coefficients and solubilities of halogenated hydrocarbons in water at ambient temperature. *Environ. Sci. Technol.* **1992**, *26*, 1828–1831.
(38) Tse, G.; Orbey, H.; Sandler, S. I. Infinite dilution activity coefficients and Henry's law coefficient of some priority water pollutants determined by relative gas chromatorgraphic method. *Environ. Sci. Technol.* **1992**, *26*, 2017–2022.
(39) Richardson, R. E.; James, C. A.; Bhupathiraju, V. K.; Alvarez-Cohen, L. Microbial activity in soils following steam treatment. *Biodegradation* **2002**, *13* (4), 285–295.
(40) Friis, A. K.; Kofoed, J. L. L.; Heron, G.; Albrechtsen, H. J.; Bjerg, P. L. Microcosm evaluation of bioaugmentation after field-scale thermal treatment of a TCE-contaminated aquifer. *Biodegradation* **2007**, *18* (6), 661–674.
(41) Gmehling, J.; Rasmussen, P.; Fredenslund, A. Vapor-liquid-equilibria by UNIFAC group contribution—Revision and extension 2. *Ind. Eng. Chem. Process Des. Dev.* **1982**, *21*, 118–127.
(42) Cooling, M. R.; Khalfaoui, B.; Newsham, D. M. T. Phase equilibria in very dilute mixtures of water and unsaturated chlorinated hydrocarbons and of water and benzene. *Fluid Phase Equilib.* **1992**, *81*, 217–229.
(43) Kuramochi, H.; Kawamoto., K. Modification of UNIFAC parameter table revision 5 for representation of aqueous solubility and 1-octanol/water partition coefficient for POPs. *Chemosphere* **2006**, *63*, 698–706.
(44) Hovarth, A. L.; Getzen, F. W.; Maczynska, Z. IUPAC-NIST solubility data series 67: Halogenated ethanes and ethenes with water. *J. Phys. Chem. Ref. Data* **2000**, *28* (2), 395–627.
(45) Adamson, D. R.; Lyon, D. Y.; Hughes, J. B. Flux and product distribution during biological treatment of tetrachloroethene dense non-aqueous phase liquid. *Environ. Sci. Technol.* **2004**, *39* (7), 2021–2028.
(46) Christ, J. A.; Abriola, L. M. Modeling metabolic reductive dechlorination in dense non-aqueous phase liquid source-zones. *Adv. Water Resour.* **2007**, *30* (6−7), 1547–1561.

ES102536F